

Preferential targeting of MCL-1 by a hydrocarbon-stapled BIM BH3 peptide

Abbas Hadji¹, Greta K. Schmitt¹, Mathew R. Schnorenberg^{1,2}, Lauren Roach¹, Connie M. Hickey¹, Logan B. Leak¹, Matthew V. Tirrell² and James L. LaBelle¹

¹Department of Pediatrics, Section of Hematology/Oncology/Stem Cell Transplantation and Committee on Cancer Biology, University of Chicago, Chicago, IL 60637, USA

²Pritzker School of Molecular Engineering, University of Chicago, Chicago, IL 60637, USA

Correspondence to: James L. LaBelle, **email:** jlabelle@peds.bsd.uchicago.edu

Keywords: MCL-1; BIM; BH3 mimetic; stapled peptides; apoptosis

Received: February 08, 2019

Accepted: October 04, 2019

Published: October 22, 2019

Copyright: Hadji et al. This is an open-access article distributed under the terms of the Creative Commons Attribution License 3.0 (CC BY 3.0), which permits unrestricted use, distribution, and reproduction in any medium, provided the original author and source are credited.

ABSTRACT

BCL-2 family proteins are central regulators of apoptosis and represent prime therapeutic targets for overcoming cell death resistance in malignancies. However, plasticity of anti-apoptotic members, such as MCL-1, often allows for a switch in cell death dependency patterns that lie outside the binding profile of targeted BH3-mimetics. Therefore discovery of therapeutics that effectively inactivate all anti-apoptotic members is a high priority. To address this we tested the potency of a hydrocarbon stapled BIM BH3 peptide (BIM SAHB_A) to overcome both BCL-2 and MCL-1 apoptotic resistance given BIM's naturally wide ranging affinity for all BCL-2 family multidomain members. BIM SAHB_A effectively killed diffuse large B-cell lymphoma (DLBCL) cell lines regardless of their anti-apoptotic dependence. Despite BIM BH3's ability to bind all BCL-2 anti-apoptotic proteins, BIM SAHB_A's dominant intracellular target was MCL-1 and this specificity was exploited in sequenced combination BH3-mimetic treatments targeting BCL-2, BCL-X_L, and BCL-W. Extending this MCL-1 functional dependence, mouse embryonic fibroblasts (MEFs) deficient in MCL-1 were resistant to mitochondrial changes induced by BIM SAHB_A. This study demonstrates the importance of understanding BH3 mimetic functional intracellular affinities for optimized use and highlights the diagnostic and therapeutic promise of a BIM BH3 peptide mimetic as a potential MCL-1 inhibitor.

INTRODUCTION

The BCL-2 family can be divided into multidomain anti-apoptotic (*e.g.* BCL-2, BCL-X_L, BCL-W, MCL-1, BFL-1) and pro-apoptotic (*e.g.* BAK, BAX) proteins. The functional interactions between these anti- and pro-apoptotic partners is controlled by a third group of proteins known as BH3-only proteins (*e.g.* BIM, BID, PUMA, BIK, BAD, NOXA, BMF) which contain one of four conserved BCL-2 homology (BH) domains. BH3-only proteins can directly bind and activate BAX/BAK or can insert their amphipathic BH3 α -helix into a groove on anti-apoptotic protein target(s) resulting in release and subsequent indirect BAX/BAK activation [1]. Cancer cells have long been known to evade cell death through overexpression of anti-apoptotic BCL-2 members

or through down-regulation of BH3-only proteins [1]. To overcome these hurdles there is a great pharmacologic crusade to develop agents that directly engage BCL-2 family proteins to induce death regardless of the cell's origin or genetic perturbations [2]. Despite early promise, many BH3-mimetics, have not effectively translated to the clinic or have been proven to work, at least in part, independent of the BCL-2 network [3–5].

Functional redundancy within the BCL-2 family can make it challenging to tailor effective therapeutic strategies without incurring resistance through upregulation of BCL-2 proteins that lie outside the mimetic's binding profile [3, 6–9]. This is exemplified by diffuse large B-cell lymphoma (DLBCL) where MCL-1 contributes to intrinsic and acquired resistance to the rationally designed polyselective BCL-2, BCL-X_L, and BCL-W inhibitor

ABT-737 and the monoselective BCL-2 inhibitor ABT-199 [10, 11]. Despite the predominance of BCL-2 protein expression in DLBCL, either through the t(14;18) translocation and/or elevated *BCL2* copy numbers, many BCL-2^{High} DLBCL are resistant to direct BCL-2 inhibition and ultimately rely on MCL-1 for survival [11]. Additionally, although activated B-cell-like (ABC) DLBCL may rely on MCL-1 to a greater extent than germinal center B-cell-like (GCB) DLBCL, protein expression alone fails to predict reliance on BCL-2 or MCL-1 in either subtype. Rather, functional sequestration of pro-apoptotic BAK and BIM appear to define sensitivity to BH3-mimetic treatment [10, 12]. The importance of releasing BIM for cell death activation is exemplified by the treatment of BCL-2^{High} DLBCL with ABT-199 or the BCL-X_L-selective inhibitor A-1155463 which results in ejection of BIM from these proteins but subsequent sequestration by MCL-1 [11]. The significance of this paradigm is reflected in encouraging results using BCL-2/BCL-X_L targeting BH3-mimetics in combination with agents that down-regulate MCL-1 in murine models of *MYC-BCL2* double-hit lymphoma and human DLBCL [13, 14]. It is clear that release of endogenous BIM sequestered by multiple anti-apoptotics is key to overcoming cell death resistance in diseases such as DLBCL.

The physiologic dominance of BIM in regulating apoptosis in hematopoietic cells is reflected in the ability of its BH3 death domain to tightly engage the BH3-binding groove of all anti-apoptotic proteins and directly activate BAX and BAK [15]. To exploit BIM's natural death-inducing functions we and others have shown that a hydrocarbon-stapled peptide modeled after the BIM BH3 α -helix (BIM SAHB_A) broadly targets BCL-2 proteins with high affinity *ex vivo*, blocks inhibitory anti-apoptotic interactions, directly triggers BAX activation, dissociates BAK from MCL-1, and induces dose-responsive and BH3 sequence-specific cell death in hematologic cancers [16–18]. In the present study, we investigated the effect of BIM SAHB_A on human DLBCL that differentially express and functionally depend on various BCL-2 anti-apoptotic proteins for survival [10]. We found that BIM SAHB_A induced apoptosis in DLBCL regardless of anti-apoptotic protein expression but that it did so most effectively in DLBCL that were increasingly resistant to ABT-737 and ABT-199. These results led to the finding that BIM SAHB_A preferentially displaced endogenous BIM from MCL-1 in these cells. Treatment with BIM SAHB_A sensitized DLBCL to ABT-737 by preventing BIM relocation onto MCL-1 following displacement from BCL-2. BIM SAHB_A's functional affinity for MCL-1 and induction of apoptosis at the level of the mitochondria was confirmed in MCL-1 deficient mouse embryonic fibroblasts (MEFs). This work highlights the importance of displacement and sequestration of BIM by anti-apoptotic BCL-2 proteins and further implicates a functional role of MCL-1 in apoptotic resistance in DLBCL. This study also illuminates the use of peptide-based BH3 mimetics

to uncover biologically relevant cell death mechanisms and confirms that functional intracellular BH3-mimetic affinities for anti-apoptotic proteins may only partially reflect their acellular binding profiles.

RESULTS

Inverse correlation between DLBCL sensitivity to BIM SAHB_A and ABT-737/ABT-199

A panel of 18 human DLBCL cell lines was treated with increasing concentrations of BIM SAHB_A, ABT-737, and ABT-199 to determine cell death as a result of distinctive anti-apoptotic targeting (Figure 1 and Supplementary Figure 1A). The cell lines were divided into 3 groups based on their ABT-737 sensitivity: ABT-737 sensitive, ABT-737 moderately sensitive, and ABT-737 resistant (Figure 1A). Our ABT-737 sensitivity profiles were similar to those previously reported using other measures of cell death, namely Annexin V positivity and ATP content [10, 11]. BCL-2 dependence in these cell lines was reflected in similar results following treatment with ABT-199 (Supplementary Figure 1A). Together, these results support increased BCL-X_L dependence in OCI-Ly10 and increased MCL-1 dependence in SU-DHL-10, HT, Pfeiffer, SU-DHL-5, SU-DHL-8, OCI-Ly7, and OCI-Ly4 cell lines as previously reported [10, 11, 17]. In contrast to treatment with ABT-737 and ABT-199, BIM SAHB_A induced dose-responsive cell death in all DLBCL cell lines with EC₅₀'s ranging from 2 μ M to 18 μ M (Figure 1B and Supplementary Table 1). Like treatment with ABT-737 and ABT-199, DLBCL could be divided into two groups based on their sensitivities to BIM SAHB_A: BIM SAHB_A 'sensitive' and BIM SAHB_A 'moderately sensitive' (Figure 1B). No death was measured in any cell line treated with a hydrocarbon-stapled BH3 point mutant control (BIM SAHB_A (R153D)) or vehicle alone indicating BIM-BH3 sequence-specific cell death induction (Supplementary Figure 1B and 1C) [16, 17, 19]. Based on our treatment analyses, there appeared to be an inverse correlation between DLBCL responses to ABT-737/ABT-199 and BIM SAHB_A (Supplementary Table 1).

BIM SAHB_A induces caspase activation in DLBCL regardless of BCL-2 family protein expression

To confirm that BIM SAHB_A treatment lead to the activation of the intrinsic apoptotic pathway and MOMP, activated caspase 3/7 was measured six hours following treatment of DLBCL with BIM SAHB_A at their individual EC₅₀ (Figure 2A). Cell death correlated with caspase 3/7 activation in all cell lines. The relative differences in caspase 3/7 activation between DLBCL may reflect differences in the kinetics of cell death in individual cell lines. Regardless, DLBCL partially or fully

resistant to ABT-737 (shown in blue and red) had similar fold caspase activation compared to ABT-737 sensitive DLBCL (shown in green) (Figure 2A). Representative cell death morphology following treatment with BIM SAHB_A displayed classical hallmarks of apoptosis such as cellular membrane blebbing, cell shrinkage, chromatin marginalization, and nuclear fragmentation consistent with previous findings (Figure 2B) [17]. No correlation existed between BIM SAHB_A-induced killing and protein expression levels of BCL-2, BCL-X_L, or MCL-1 (Figure 2C and Supplementary Figure 2A–2C). This is similar to other reports where no correlations were measured between protein expression of BCL-2 and BCL-X_L and DLBCL responses to ABT-737 or ABT-199 [10, 11]. There was also no correlation in apoptosis and levels of other BCL-2 proteins known to be associated with cell death resistance in B-cell lymphomas including BIM, BID, PUMA, BAX, or BAK (Supplementary Figure 2D–2H) [10, 12, 20–23]. Given the importance of release of BIM for apoptosis induction in DLBCL, these results suggested

that BIM SAHB_A was able to block endogenous BIM binding to MCL-1, BCL-2 and/or BCL-X_L expressing cells regardless of their sensitivity to ABT-737/ABT-199.

BIM SAHB_A dissociates BIM from MCL-1 to a greater extent than BCL-2

We next sought to investigate the ability of BIM SAHB_A to release endogenous BIM from BCL-2 or MCL-1 in DLBCL that were sensitive (OCI-Ly1 > SU-DHL-6 > OCI-Ly8) or resistant (SU-DHL-5) to ABT-737 (Figure 1A, Supplementary Table 1) [10, 11]. The three ABT-737 sensitive cell lines were chosen as they represent an array of DLBCL phenotypes based on predominant anti-apoptotic BCL-2 family member expression (*e.g.* BCL-2, BCL-X_L, and MCL-1). Importantly, these DLBCL depend, even if partially, on BCL-2, rather than BCL-X_L for cell death control [10, 13]. Treatment of individual cell lines with the EC₅₀ of either ABT-737 or BIM SAHB_A alone was followed by immunoprecipitation of BCL-2 and MCL-1

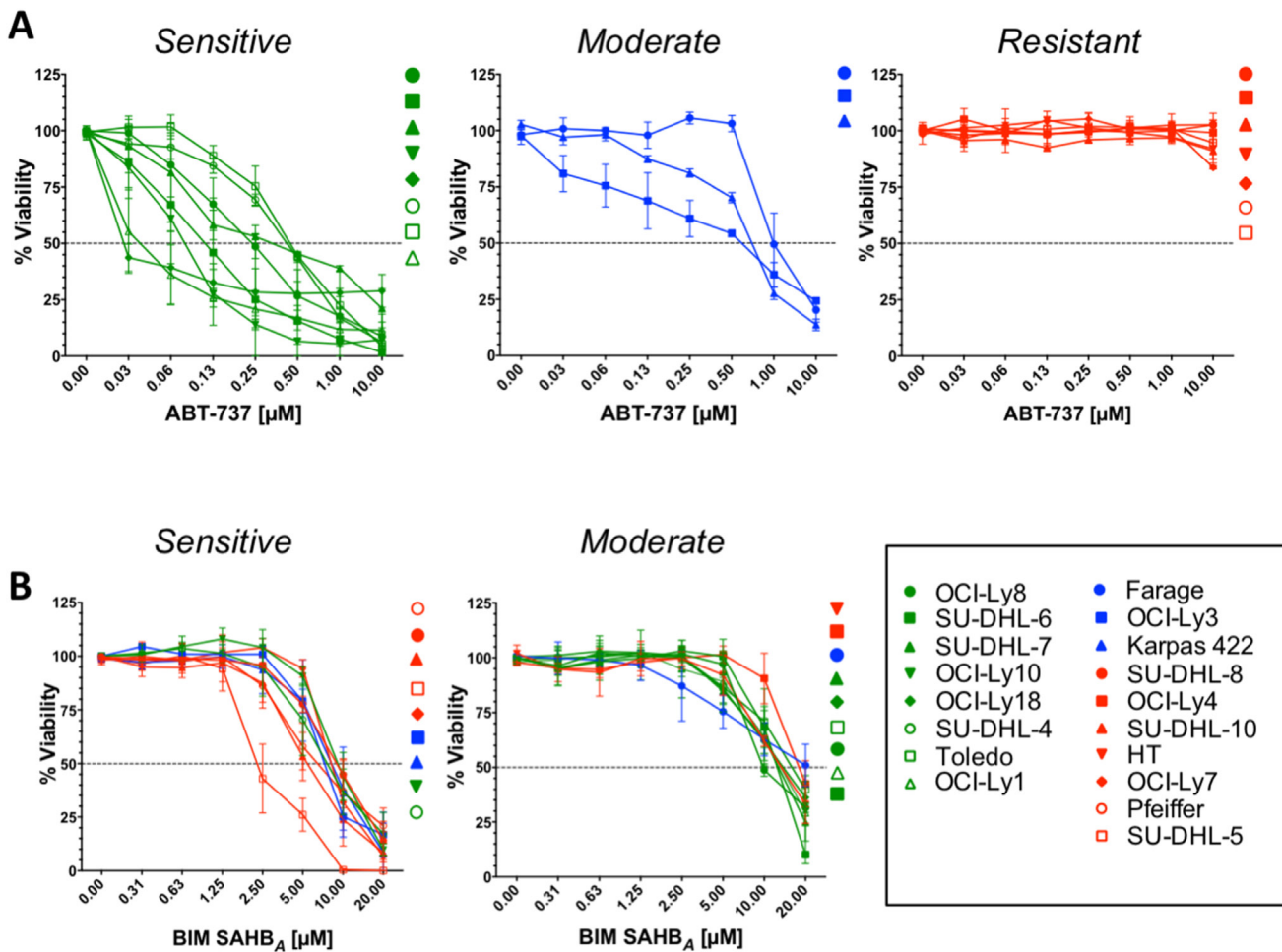


Figure 1: Sensitivity of DLBCLs to BIM SAHB_A inversely correlates with their sensitivity to ABT-737. Cell viability in a panel of human DLBCL cell lines was measured after 24-hr incubation with increasing concentrations of (A) ABT-737 or (B) BIM SAHB_A. Percent (%) viability was calculated as a percentage of control (DMSO) treated cells. Dose-response curves indicating highest sensitivity to ABT-737 are in green, those indicating moderate sensitivity to ABT-737 are in blue, and those indicating low to no sensitivity to ABT-737 are in red. Error bars are mean \pm SEM for at least three independent preparations of cell and BH3 mimetic treatments.

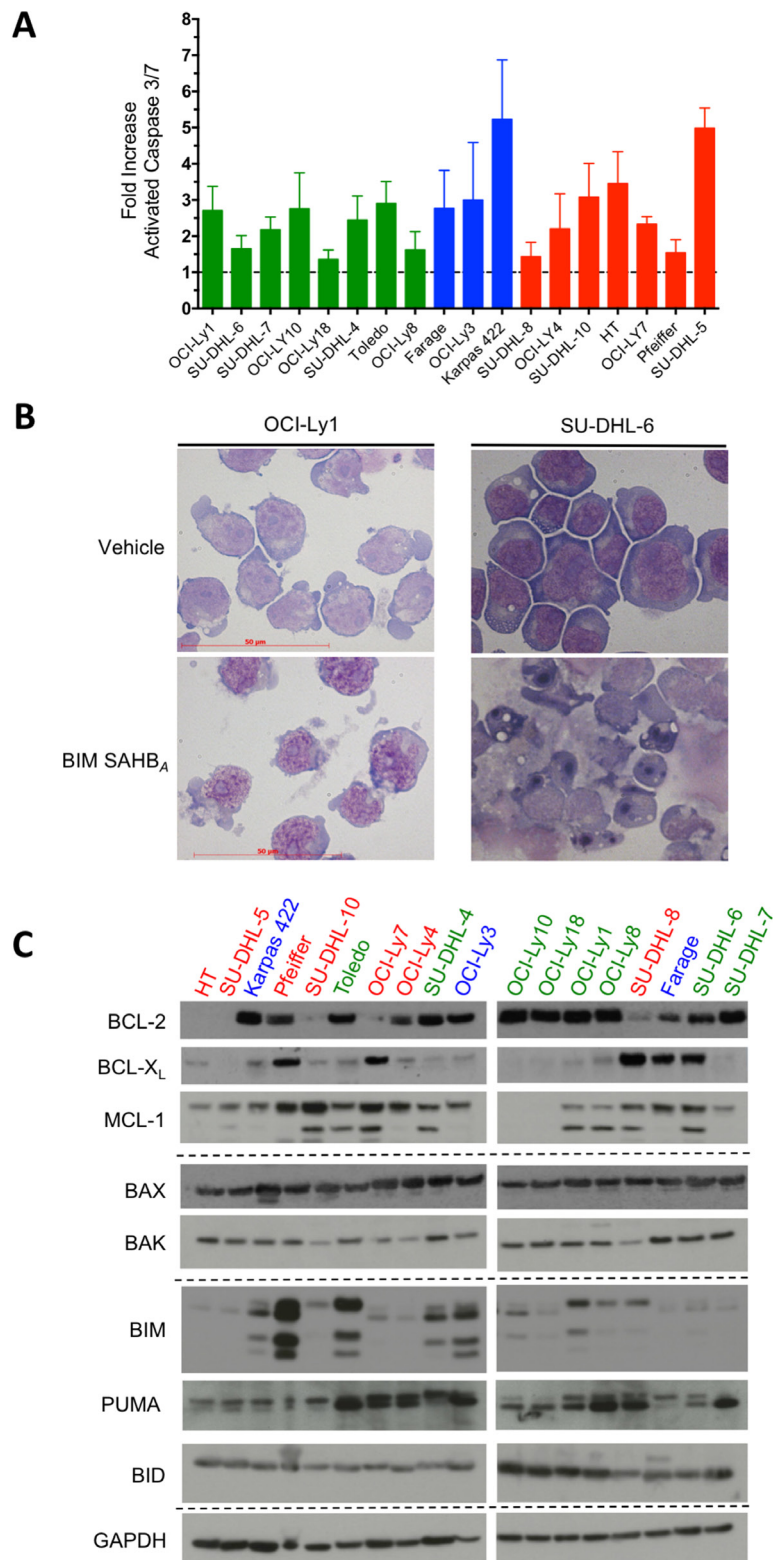


Figure 2: BIM SAHB_A treatment results in caspase 3/7 activation and cellular hallmarks of apoptosis irrespective of BCL-2 family protein expression in DLBCL. (A) DLBCL cell lines were treated BIM SAHB_A at their respective EC₅₀ for 6-hr and activation of the intrinsic apoptotic pathway was assessed by monitoring the cleavage of pro-luminescent caspase 3/7 substrate. Caspase activity was calculated as fold change as compared to control (DMSO) treated cells. (B) BIM SAHB_A-treatment results in hallmarks of apoptosis such as cellular membrane blebbing, cell shrinkage, chromatin marginalization, and nuclear fragmentation. (C) Western blot analysis of BCL-2 proteins in DLBCL cell lines. Colors of each cell line reflect their ABT-737 sensitivity patterns as depicted in Figure 1 and Supplementary Figure 1. Error bars are mean ± SEM for at least three independent preparations of cell and BIM SAHB_A treatments.

and immunoblotting for endogenous BIM. As expected, treatment with ABT-737 resulted in dissociation of BIM from BCL-2 in BCL-2- expressing DLBCL (Figure 3). Once dissociated, BIM became sequestered by MCL-1, as measured particularly in OCI-Ly8 and SU-DHL-6 cells where the MCL-1:BIM complex following treatment with ABT-737 was greater than control treated cells (Figure 3A and 3C). In contrast, treatment with BIM SAHB_A led to measurable, but minimal, displacement of endogenous BIM from BCL-2 in comparison to ABT-737. BIM SAHB_A treatment resulted in much greater dissociation of BIM from MCL-1 with no detectable increased accumulation on BCL-2 in all three cell lines (Figure 3). Thus, although BIM SAHB_A was better able to dissociate endogenous BIM from MCL-1, it was still able to prevent redistribution of BIM to BCL-2 [17]. Given these results, we were interested if step-wise treatment with ABT-737 and BIM SAHB_A resulted in improved dissociation of BIM from either BCL-2 or MCL-1 and blockage of subsequent binding of released BIM on the alternate anti-apoptotic protein. To test this, cells were treated with either ABT-737 or BIM SAHB_A for three hours followed by addition of the other compound (*i.e.* ABT-737 + BIM SAHB_A or BIM SAHB_A + ABT-737). BIM SAHB_A was unable to release relocated BIM from MCL-1 that was dissociated from BCL-2 upon treatment first with ABT-737 (Figure 3). The increased BIM:MCL-1 association following treatment with ABT-737 overwhelmed the ability of BIM SAHB_A to effectively target MCL-1 at the same doses used during monotherapy. However, treatment with BIM SAHB_A before ABT-737 led to relocation of BIM from both BCL-2 and

MCL-1. This phenomenon was greatest in OCI-Ly8 and SU-DHL-6 (Figure 3A and 3C) [10, 13]. In fact, although monotherapy of SU-DHL-5 and OCI-Ly1 with BIM SAHB_A led to release of endogenous BIM from MCL-1, this effect was largely lost in both combination treatments (Figure 3B and Supplementary Figure 3A) [24, 25]. There were no gross differences in expression of BCL-2, MCL-1, or BIM during the six hour treatment timeframe in any cell line following individual or combination treatments (Supplementary Figure 4). Dissociation of BAK from MCL-1 and activation of BAX in these cell lines may also have played a role in cell death following BIM SAHB_A treatment as has been reported previously [17, 26]. Dissociation of BAX from BCL-2 also occurs in these cell lines following treatment with both ABT-737 and BIM SAHB_A (Supplementary Figure 5).

BIM SAHB_A sensitizes DLBCL to ABT-737

To test if sequential treatment would lead to differential effects on cell viability, DLBCL were treated as above and cell death was measured after 24 hours. Consistent with the BIM relocation results (Figure 3 and Supplementary Figure 3A) treatment with BIM SAHB_A prior to ABT-737 led to increased cell death when compared to the opposite treatment or monotherapy with either compound (Figure 4 and Supplementary Figure 3B). Equivalent results were measured when cells were treated with ABT-737 alone or with ABT-737 followed by BIM SAHB_A as was predicted by our BIM relocation data. The largest effect was measured in OCI-Ly8 correlating with

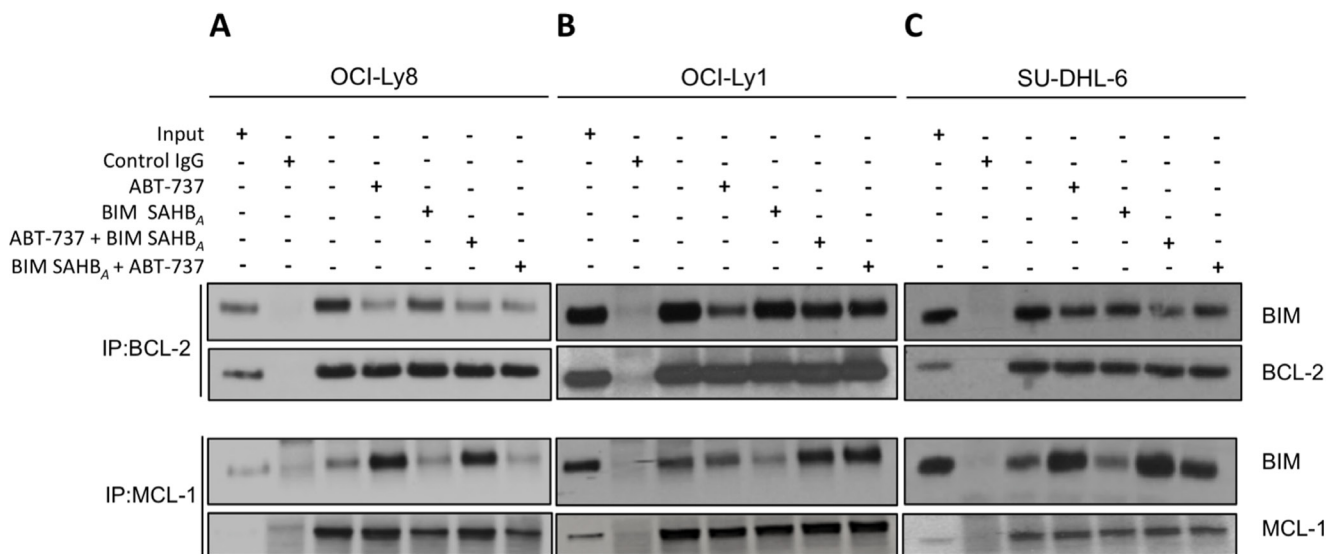


Figure 3: BIM SAHB_A preferentially targets MCL-1 over BCL-2 in ABT-737-sensitive DLBCL. (A) OCI-Ly8, (B) OCI-Ly1, and (C) SU-DHL-6 were left untreated (third lane) or treated with ABT-737 (EC₅₀; fourth lane), BIM SAHB_A (EC₅₀; fifth lane), ABT-737 for three hours followed by BIM SAHB_A for three hours (sixth lane), or BIM SAHB_A for three hours followed by ABT-737 for three hours (seventh lane). Lysates were immunoprecipitated with antibodies specific for BCL-2, MCL-1, or anti-Rabbit IgG (control), and immune complexes were resolved and immunoblotted for BIM, BCL-2 and MCL-1. Input lysate was loaded in the first lane and immunoprecipitates with a control IgG in the second lane. Treatments: OCI-Ly8: ABT-737 241 nM, BIM SAHB_A 13.2 μM; OCI-Ly1: ABT-737 30.7 nM, BIM SAHB_A 12 μM; SU-DHL-6: ABT-737 113 nM, BIM SAHB_A 12 μM.

BIM SAHB_A's ability to fully block BIM sequestration on MCL-1 following treatment with ABT-737 (Figure 4C). Regardless of overall effect, treatment with BIM SAHB_A prior to treatment with ABT-737 at a ratio of 10:1 universally led to increased cell death when compared to the reverse treatment in all cell lines (ABT-737 EC₅₀: OCI-Ly8: 165 nM to 40.1 nM (76% decrease); OCI-Ly1: 93 nM to 66.4 nM (29% decrease); SU-DHL-6: 100 nM to 63.5 nM (37% decrease); and SU-DHL-5: >10,000 nM to 3,360 nM (~66% decrease) (Figure 4A–4C and Supplementary Figure 3B). In each case, synergy was observed when BIM SAHB_A was given prior to ABT-737, as reflected by combination indices of less than 0.8 at 50%, 75%, and 90% effective doses. Apart from synergy in OCI-Ly1, ABT-737 treatment prior to BIM SAHB_A predominantly resulted in an additive cell killing effect with combination indices between 0.8 and 1.1 [27]. These effects were magnified in OCI-Ly8 at a BIM SAHB_A:ABT-737 ratio of 20:1 where the EC₅₀ decreased from 165 nM to 32.2 nM (80% decrease) and synergy was increased at all effective doses indicating that the amount of BH3 mimetic may play a role in sequential dosing but does not significantly alter synergy values (Figure 4D). The increased sensitivity to ABT-737, particularly in OCI-Ly8, correlated with the ability of MCL-1 to absorb redistributed BIM once released from BCL-2 in these cells. Our results align with previous work showing that normal lymphoid cell and human non-Hodgkin lymphoma resistance to ABT-737 is conferred by mutant BIM specific for BCL-2, BCL-X_L, and BCL-W [28]. However, mutant BIM specific for MCL-1 led to ABT-737 sensitivity indicating that ABT-737-mediated killing only occurred when MCL-1 was neutralized [28]. Our data would suggest that BIM SAHB_A is more selective for intracellular MCL-1 and effectively prevents BIM:MCL-1 association in a similar context.

To identify and correlate relevant BCL-2 pro-survival dependency in cells with either high (OCI-Ly8) or low (OCI-Ly1) MCL-1:BIM binding following ABT-737 treatment, we employed lentiviral expression of BIM_S-derived BH3 variants [29]. These variants can determine biologically relevant BH3-only protein dependence within an intact cellular environment [30]. OCI-Ly8 and OCI-Ly1 were engineered to inducibly express: 1) BIM_SWT able to target all pro-survival proteins, 2) BIM_S2A able to target MCL-1 only, 3) BIM_SBAD able to target BCL-2, BCL-X_L and BCL-W; or 4) BIM_S4E unable to bind any anti-apoptotic, serving as a negative control (Supplementary Figure 6) [29]. BIM_SWT expression greatly reduced the viability of both OCI-Ly8 and OCI-Ly1. OCI-Ly8 cells were more sensitive to BIM_SBAD compared to BIM_S2A indicating more BCL-2 dependence. This anti-apoptotic dependency pattern supports the increased cell death in OCI-Ly8 when treated first with BIM SAHB_A followed by ABT-737 where BIM, released from BCL-2 was unable to reoccupy itself on MCL-1 (Figure 4C). In contrast, targeting of

MCL-1 by BIM_S2A in OCI-Ly1 led to cell death equal to that of BIM_SWT while the response to BIM_SBAD was more moderate (Supplementary Figure 5B). Thus, OCI-Ly1 was overall more sensitive to BIM expression in this setting and more dependent on MCL-1 than BCL-2, supporting a different sequestration dynamic when endogenous BIM is dissociated from MCL-1 following BIM SAHB_A treatment. This is despite both DLBCL having similar baseline expression of BCL-2 (Supplementary Figure 2) [10, 11]. Together, these results support that the preferential intracellular target of BIM SAHB_A was MCL-1.

MCL-1 is required for BIM SAHB_A-dependent defects in the outer mitochondrial membrane

Mouse embryonic fibroblasts (MEFs) are dependent upon MCL-1, and to a lesser extent, BCL-X_L, for survival [31]. MCL-1 plays the more critical functional role in regulating apoptosis as reflected by the ability of ABT-737 to induce apoptosis only in MCL-1-deficient MEFs [9, 31]. We have previously shown that BIM SAHB_A can induce apoptosis in MCL-1-dependent and ABT-737-resistant malignant hematopoietic cells lines and can dissociate BAK from MCL-1 [17]. We have also shown that BIM SAHB_A can induce cell death in WT MEFs but not in BAX^{-/-}BAK^{-/-}MEFs [16, 17]. To investigate the general dependence on MCL-1 for BIM SAHB_A-induced cell death we used MCL-1^{-/-} MEFs and MEFs with inducible deletion of MCL-1 (Mcl-1^{fl/fl} Rosa-ERCreT2 MEFs) to ensure there was no BCL-2 family compensation secondary to long-term MCL-1 loss [32]. WT and WT Rosa-ERCre T2 MEFs had equivalent expression of MCL-1 and MCL-1 protein was not detectable in either MCL-1^{-/-} or Mcl-1^{fl/fl} Rosa-ERCreT2 MEFs following treatment with tamoxifen (Figure 5A). Loss of MCL-1 in either MEF allowed for significant apoptosis in response to treatment with ABT-737 (Supplementary Figure 7). ABT-737 induced greater death in Mcl-1^{fl/fl} Rosa-ERCreT2 MEFs compared to MCL-1^{-/-} MEFs likely because MCL-1^{-/-} MEFs have developed BCL-2 compensatory mechanisms through long-term culturing as has been previously documented in genetic knockout model systems [33, 34]. In contrast to ABT-737, BIM SAHB_A induced death in both WT MEFs while either long-term or short-term absence of MCL-1 led to equivalent protection (Figure 5B). Only loss of MCL-1 was responsible for resistance to BIM treatment as indicated by equivalent cell death in MCL-1^{-/-} or Mcl-1^{fl/fl} Rosa-ERCreT2 MEFs.

We extended these results to investigate if treatment with BIM SAHB_A caused MCL-1-dependent changes in mitochondria morphology. Treatment of WT MEFs with BIM SAHB_A led to cristae disorganization and mitochondrial swelling, hallmarks of intrinsic apoptotic pathway activation (Figure 6A) [35, 36]. These phenotypic changes were not evident in treated MCL-1^{-/-} MEFs

indicating that BIM SAHB_A preferentially targets MCL-1 in these cells (Figure 6B). These phenotypic data confirm BIM SAHB_A's ability to target intracellular MCL-1 and supports an MCL-1-dependent mechanism responsible for sensitivity to BIM SAHB_A [17].

DISCUSSION

The presence of BCL-2 family anti-apoptotic members dictates cellular sensitivity to BH3 mimetics. However, expression alone is not enough to predict apoptotic functional dependency patterns, especially as it relates to malignant cell death. This is particularly evident in cells where expression of BCL-2, BCL-X_L, or BCL-W does not always result in sensitivity to ABT-737 [37–41]. Additionally, *ex vivo* sensitivity against these agents does not always correlate with long-term *in vivo* results either in pre-clinical human xenograft studies or in patients

[25, 39]. A primary reason for these resistance patterns is the up-front presence or emergence of MCL-1 during the course of treatment confirming the dynamism of the BCL-2 family regulatory network [42–44]. Importantly, despite the ability of ABT-737, or its oral analogue ABT-263, to bind BCL-2, BCL-X_L, and BCL-W, it appears to overwhelmingly bind BCL-2 even when the other anti-apoptotics are present [28, 45]. A recent example of this preferential intracellular attraction is that treatment with ABT-199 or a BCL-X_L-specific mimetic induced more cell death in BCL-2 and BCL-X_L expressing human small cell lung cancer (SCLC) and AML cell lines than treatment with ABT-263, indicating an intracellular preference for either BCL-2 or BCL-X_L, but not both, by ABT-263 [46]. This phenomenon extends to *in vivo* testing in SCLC xenograft models where combination treatment with ABT-199 and the BCL-X_L-specific mimetic resulted in better survival than treatment with ABT-263 alone [46].

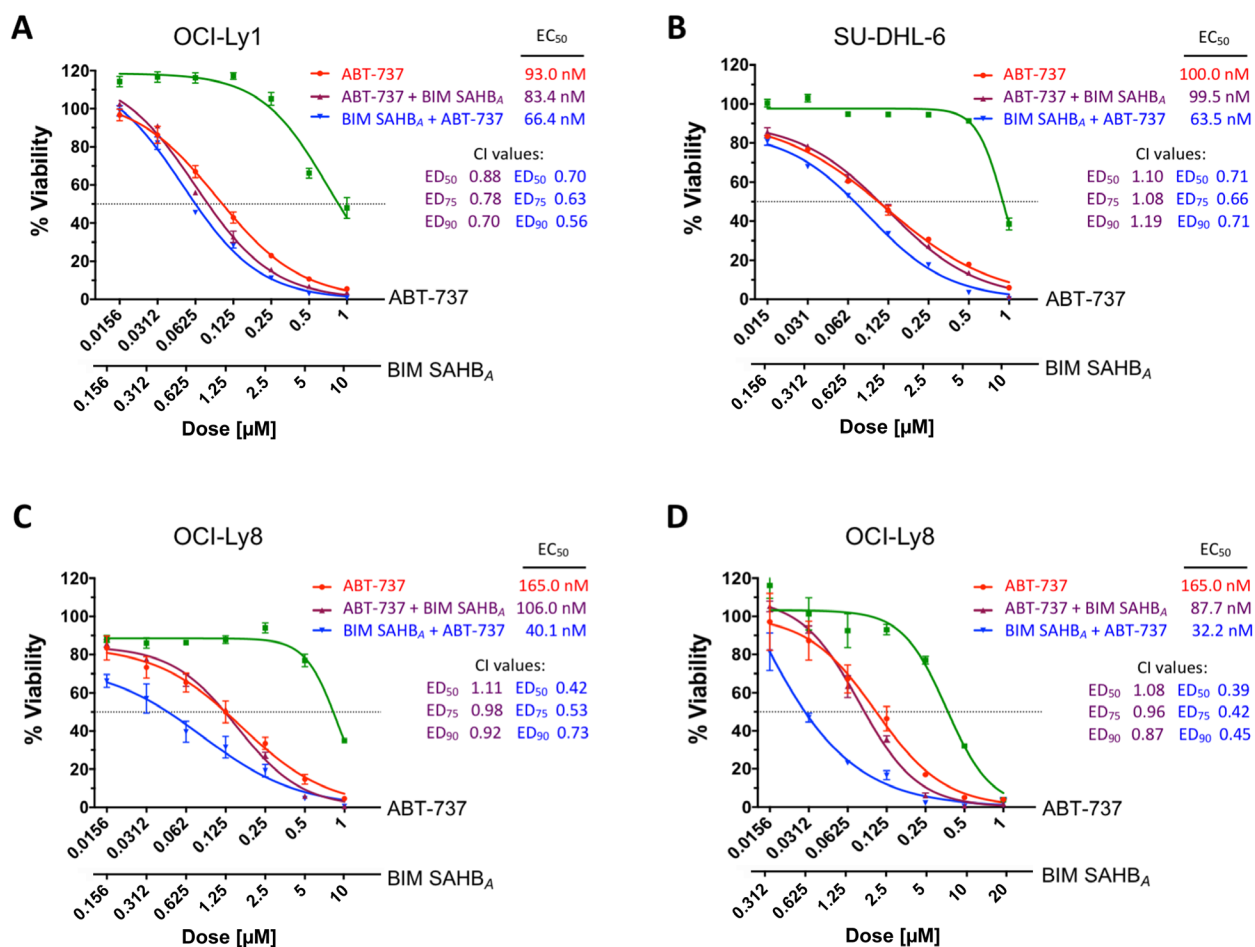


Figure 4: Treatment with BIM SAHB_A increases DLBCL cell death when given before but not following treatment with ABT-737. Cell viability of (A) OCI-Ly1, (B) SU-DHL-6, and (C, D) OCI-Ly8 was measured after 24-hr treatment with increasing concentrations of ABT-737 (red), BIM SAHB_A (green), ABT-737 for the first three hours followed by BIM SAHB_A (purple), or BIM SAHB_A for the first three hours followed by ABT-737 (blue). BIM SAHB_A given prior to ABT-737 universally led to a greater synergistic decrease in cell viability, as reflected by CalcuSyn analysis (combination index [CI] <1). Error bars are mean ± SEM for at least three independent preparations of cells and BH3 mimetic treatments. EC₅₀, 50% effective concentration; ED₅₀, 50% effective dose; ED₇₅, 75% effective dose; ED₉₀, 90% effective dose.

Adding to the difficulty in navigating the BCL-2 targeting landscape, cancers derived from the same cell type can show different BCL-2 anti-apoptotic dependencies [10, 40, 41, 46, 47]. These differences often relate to levels of BIM expression and patterns of BIM:anti-apoptotic sequestration [47]. DLBCL is an example of such a disease where cell death resistance depends upon combinations of BIM bound to a number of antiapoptotics (BCL-2, BCL-X_L, and MCL-1), and is therefore a useful model for testing the importance of both anti-apoptotic expression and BIM:anti-apoptotic sequestration differences relating to BH3-mimetic sensitivity [10–12, 25].

Like other BH3 mimetics, quantitative expression levels of BCL-2 proteins alone were not effective

indicators of sensitivity to BIM SAHB₄. However, given the natural affinity of the BIM BH3 death domain to engage all anti- and pro-apoptotic BCL-2 proteins, it was not surprising that the cell permeable hydrocarbon-stapled BIM BH3 therapeutic reactivated cell death in all DLBCL tested. The ability of BIM SAHB₄ to displace endogenous BIM from BCL-2 and MCL-1 supports the promise of the BIM BH3 domain as a therapeutic. Unexpectedly, like ABT-737/ABT-263 intracellular affinity for BCL-2 in many disease models, BIM SAHB₄ has a propensity for targeting intracellular MCL-1 over BCL-2. This was likely responsible for its inverse sensitivity profile against the DLBCL cell lines compared to that of ABT-737 and ABT-199. In this regard, a therapeutic with BIM SAHB₄'s

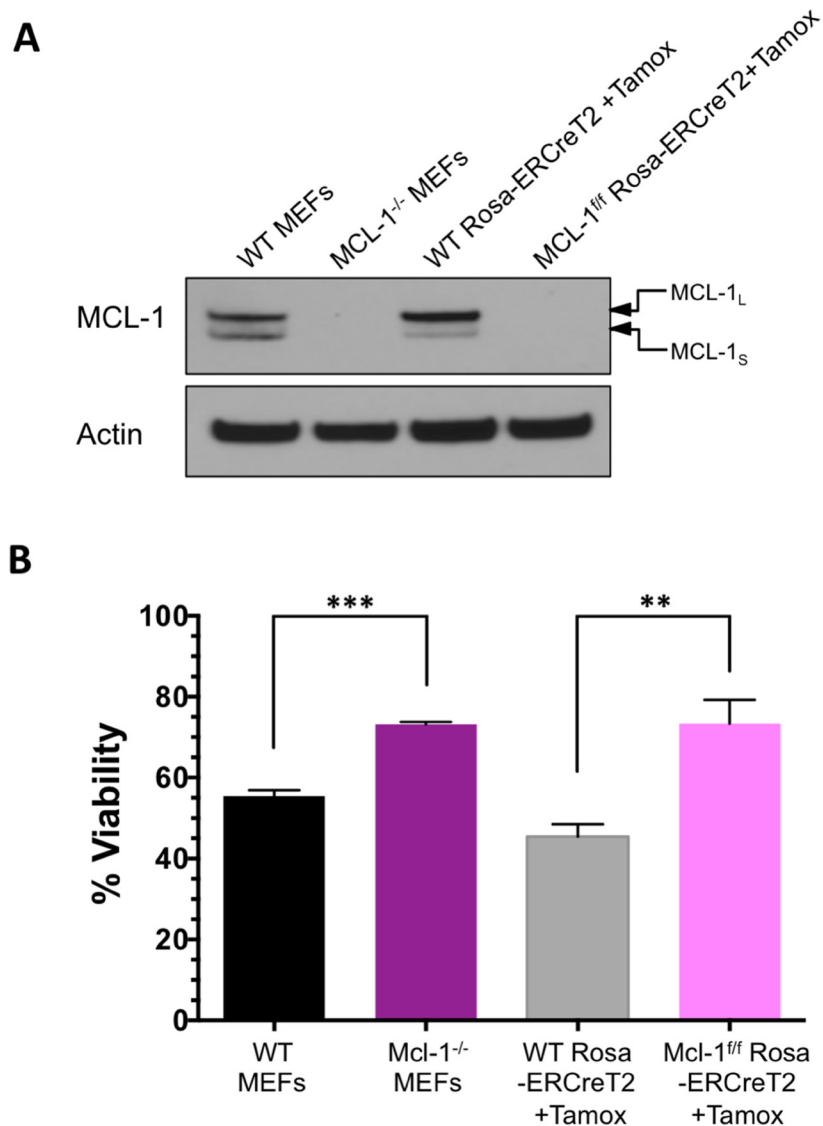


Figure 5: Absence of MCL-1 leads to resistance against BIM SAHB₄-induced apoptosis. (A) Western blot analysis of MCL-1 expression in WT MEFs and MCL-1^{-/-} MEFs at steady-state and Rosa-ERCreT2 control MEFs and Mcl-1^{ff} Rosa-ERCreT2 MEFs 72-hr following treatment with 100 nM of (4-hydroxy)-tamoxifen. Equivalent presence of MCL-1 was measured in the control MEFs and complete loss of MCL-1 was measured in MCL-1^{-/-} and Mcl-1^{ff} Rosa-ERCreT2 MEFs. Short (S) and long (L) isoforms of MCL-1 are indicated by arrows. (B) Cell viability of these MEFs was measured following 24-hr treatment with 20 μM BIM SAHB₄. Error bars are mean ± SEM for at least three independent preparations of cells and BH3 mimetic treatments.

therapeutic profile could be of particular benefit against activated B-cell like (ABC) DLBCLs that express *MCL1* at higher levels and have higher MCL-1:BIM binding than germinal center B-cell like (GCB) DLBCL [12]. However, despite the single agent efficacy of BIM SAHB_A against DLBCL as shown here, combination BH3 mimetic therapy will likely be necessary for reactivation of cell death at clinically useful levels [47–49]. Our data would also suggest that dosing and the sequence of such therapies are critical.

We found that BIM SAHB_A was unable to effectively dissociate a large amount of released endogenous BIM following treatment with ABT-737 when MCL-1 was present. However, prior to release from BCL-2, BIM SAHB_A was able to efficiently bind MCL-1 and prevent

relocation of BIM in the more BCL-2-dependent and lower MCL-1 expressing cell lines (Figure 3A and 3C). It should be noted that DLBCL were treated at their EC₅₀ in our study so as to capture cells before they underwent complete apoptosis. Additional studies will be needed to determine if increased doses of BIM SAHB_A, as used in Figure 4D, or various treatment times would adequately remove BIM from DLBCL with larger amounts of MCL-1 following treatment with ABT-737 or ultimately stabilize MCL-1 protein levels as do newly introduced high-affinity small molecule MCL-1 inhibitors [6, 50]. In addition to dosing amounts, the timing of death induced by such treatments, either alone or in combination, likely differ between cell lines. Such differences could also be reflected in the relative amount of caspase 3/7 activation

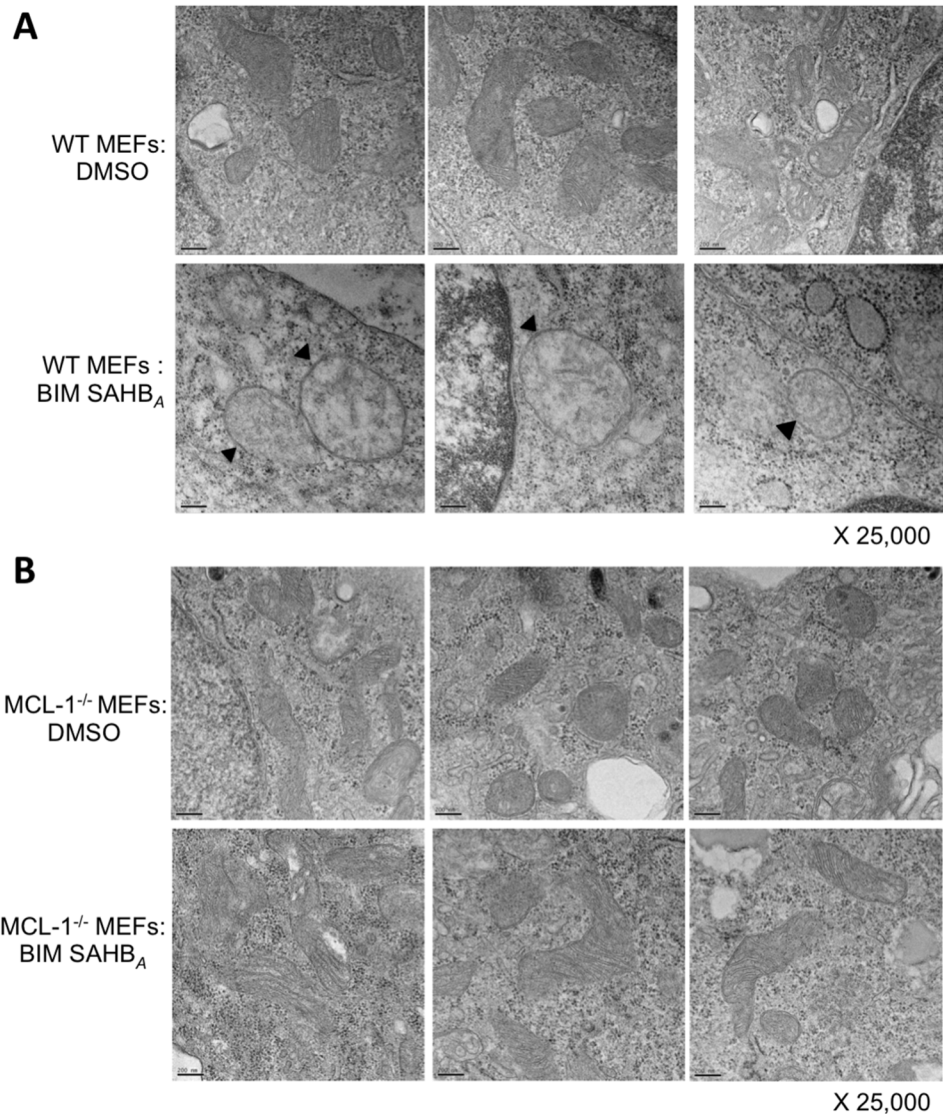


Figure 6: BIM SAHB_A induces characteristic hallmarks of apoptosis at the level of the mitochondria in the presence of MCL-1. (A) WT MEFs treated for 6-hr with DMSO (control; upper panels) or 20 μM BIM SAHB_A (lower panels) were monitored for mitochondrial apoptotic morphology using electron microscopy. (B) Identical treatment and imaging was performed on MCL-1^{-/-} MEFs. Black arrowheads point to mitochondrial swelling and loss of cristae architecture in BIM SAHB_A-treated WT MEFs but not in MCL-1^{-/-} MEFs revealing a dependence on MCL-1 for BIM SAHB_A-mediated apoptosis. x 25,000 magnification; scale bars, 200 nm.

(Figure 2A) or synergy calculations in these and other cell lines where such combination treatments have been tested [11, 13, 14, 51]. Additionally, this work does not rule out the possibility of simultaneous triggering of caspase-dependent (*e.g.* apoptosome/caspase 3 and endonuclease activity) and caspase-independent (*e.g.* AIF) pathways following BIM SAHB₄ treatment and caspase 3/7 activation. Despite this, the current study reinforces work indicating that the ability of BH3-mimetics to preferentially target intracellular BCL-2 anti-apoptotic members often does not completely reflect their *in vitro* binding profile(s) [4, 10, 28, 45]. We and others have shown that BIM SAHB₄ binds MCL-1, BCL-X_L, BCL-2, and A1 with low nanomolar affinity and is able to dissociate BAK and BAX BH3 ligands from MCL-1 and BCL-X_L respectively [17, 52]. Although able to bind all anti-apoptotics tested, the current study supports that the preferential intracellular target of BIM SAHB₄ is MCL-1 over BCL-2, at least in DLBCL. However, we cannot discount that direct activation of BAX or dissociation of other BH3-only proteins, such as BID, plays a role in the overall cell death effectiveness of BIM SAHB₄ in these same cells [16, 17, 26, 52].

Well-timed combination BH3 mimetic therapy may be a promising strategy against diseases like DLBCL where oncoproteins (*e.g.* MYC, BCL6, and BCL-2) play roles in blocking the intrinsic apoptotic network through direct upregulation of BCL-2 family members and other cell death-related proteins [53, 54]. Such complex perturbation in apoptotic regulation necessitates a combinatorial therapeutic approach involving multiple BH3 mimetics, which may include small molecule and peptide-based therapeutics, alone or with other conventional chemotherapies. A complete understanding of intracellular affinities and the therapeutic ramifications of targeted anti-apoptotic therapeutics on relocation of BIM will be critical as BH3-mimetic therapies are advanced.

MATERIALS AND METHODS

Cell culture and therapeutic reagents

Human DLBCL cell lines (kind gift from Margaret A. Shipp, M.D., Dana-Farber Cancer Institute, Boston, MA 02115, USA and purchased from ATCC and DSMZ) were cultured in RPMI 1640 medium supplemented with 0.5 mg/ml penicillin/streptomycin, 2 mM L Glutamine, 1 mM HEPES, Non-Essential Amino Acids (all from Life technologies) and 10% heat inactivated fetal bovine serum (*Denville Scientific*). HEK293T were obtained from American Type Culture Collection. HEK293T cells and MEFs Cells were grown in Dulbecco's modified Eagle's medium (DMEM, Life technologies) supplemented with same reagents as previously mentioned. For BIM SAHB₄ treatment, cells were cultured in advanced RPMI

supplemented with 0.5 mg/ml penicillin/streptomycin, 2 mM L Glutamine, 1 mM HEPES, 1% NEAA. All cells were maintained at 37°C in 5% CO₂. Wild-type ERCreT2 and Mcl-1f/f Rosa-ERCreT2 MEFs were a kind gift from Joseph T. Opferman Ph.D., St. Jude Children's Research Hospital. BIM SAHB₄ and BIM SAHB₄ (R153D) were synthesized, purified, as previously reported [16, 17, 19]. SAHB constructs used in caspase assays and confocal cell death assays were a kind gift from Loren D. Walensky, M.D., Ph.D. and Gregory Bird, Ph.D., Dana-Farber Cancer Institute, Boston, MA. All other SAHBs used for cell treatments were synthesized at the University of Chicago. Doxycycline (Sigma), ABT-199 (Selleck Chemicals), ABT-737 (Selleck Chemicals), (4-hydroxy)-tamoxifen (Sigma).

Viability assays

DLBCL (2 × 10⁴ cells) were treated with serial dilutions of BIM SAHB₄, ABT-199, ABT-737 or DMSO for 2 h in serum free advanced RPMI media followed by addition of FBS to the media (to 10% [v/v]) as previously described [17]. Viability was assessed using Cell proliferation kit II XTT (Roche) according to the manufacturer's instructions. Absorbance EC₅₀s were calculated using GraphPad Prism 6 software. For combination treatments, DLBCL (2 × 10⁴ cells) were treated with serial dilutions of BIM SAHB₄ (0–20 μM) or ABT-737 (0–1 or to 20 μM), 3 h in serum free advanced RPMI media followed by 3 h of treatment with either ABT-737, BIM SAHB₄ or DMSO (0.2%). FBS was then added to the media (to 10% [v/v]). Viability was assessed 24 h later using CellTiter-Glo according to the manufacturer's instructions. (XTT) or luminescence (CellTiter-Glo) was detected by Synergy 2 microplate reader (BioTek). Synergy analyses were performed as previously described [17].

Caspase-3/7 activation assay

DLBCL (10,000 cells/well) were seeded in 96-well plates in advanced RPMI Growth Media and were treated with BIM SAHB₄ or DMSO for 6 hours. Caspase-Glo 3/7 chemiluminescence reagent (Promega) was used according to manufacturer's directions. Luminescence was measured by a Synergy 2 microplate reader (BioTek) and was standardized to DMSO treated samples as previously described [17].

Western blot analysis

Following treatment of individual DLBCL with compounds, cells were washed with PBS and lysed in cell lysis buffer (25 mM HEPES pH 7.5, 150 mM NaCl, 1% Triton X-100, 0.1% SDS, 5 mM EDTA and 1 mM NaF supplemented with 1x protease inhibitor cocktail tablets [Roche]) as previously described [17]. Protein concentrations were determined by Pierce BCA Protein

Assay Kit (Thermo Scientific). 30 µg of protein were electrophoretically separated on NuPAGE 12% Bis-Tris polyacrylamide gels (Invitrogen). Separated proteins were transferred to nitrocellulose membranes (BioRad). Blots were incubated with the following antibodies: MCL-1 (Santa Cruz, S-19), BCL-2 (Epitomics, 1017-1), BCL-X_L (Santa Cruz, S18), BIM (Millipore AB17003), BAX (Santa Cruz, N20), BAK (Millipore 06-536), BID (Santa Cruz), GAPDH (Santa Cruz FL-335), PUMA (Santa Cruz). The immune complex was detected using anti-rabbit HRP-conjugated antibody (Envision Detection Kit, DakoCytomation) and the chemiluminescent detection kit according to the manufacturer's specifications (Amersham). Proteins were visualized with *CL-XPosure Film* (Thermo Scientific) using AX200 X-Ray film processor (Aphatek).

Immunoprecipitation

DLBCL (9×10^6 cells) were lysed in 2 ml of Triton X-100 buffer (50 mM Tris-HCL [pH 7.4], 150 mM NaCl, 5 mM MgCl₂, 1 mM EGTA, 10% Glycerol, 1% Triton X-100 and 1x protease inhibitor cocktail tablets [Roche]) on ice for 30 min and then centrifuged at 18,000 × g for 20 min at 4°C. 400 µg proteins was pre-cleared using 30 µl of Pierce Protein A Magnetic Beads (Thermo Scientific) for 2 hours at 4°C then incubated overnight at 4°C with MCL-1 antibody (Protein Tech, 16225), BCL-2 antibody (Epitomics, 1017-1) or Rabbit IgG. 20 µl of Magnetic beads were added and incubated for 2 hours. Immunoprecipitates were then washed 5 times with 500 µl of Triton X-100 buffer and boiled in *NuPAGE LDS Sample Buffer* (Thermo Scientific) supplemented with 1 mM DTT and proteins were separated on NuPAGE 10% Bis-Tris polyacrylamide gels.

Wright-giemsa stain

DLBCL cells were treated with vehicle or BIM SAHB_A in Opti-MEM media for 4 hours at 37°C. Cells stained as previously described [17]. Briefly, cells were collected and washed twice with PBS containing 2% FBS and resuspended at 2.5×10^6 cells/ml for mounting of the cellular suspension onto glass slides by cytospin. The slides were air dried and then stained with Accustain Modified Wright-Giemsa according to the manufacturer's protocol (Sigma-Aldrich).

BIM_s isoform lentivirus production and transduction

The TRIPZ vectors with inducible expression of the different variants of BIM_s were a kind gift from Andreas Strasser, Ph.D. (The Walter and Eliza Hall Institute, Parkville, Melbourne) [29]. To generate cells stably expressing the inducible BIM_s variants, DLBCL cells were infected with viral supernatants, produced by lipofectamine 2000 co-transfection of 293T cells with

TRIPZ expression constructs and packaging plasmids according to the manufacture protocol and as previously described [29]. Cells were expanded then FACS-sorted for the expression of GFP using a *BD FACSAria* cell sorter. The expression of BIMs proteins was induced as previously described [29].

Electron microscopy

Indicated MEFs were plated in six-well format (2×10^5 cell/condition) were washed in serum free Advanced DMEM following overnight induction. The cells were then incubated with 20 µM BIM SAHB_A or vehicle (0.05% [v/v] DMSO) for 2-hr, and then FBS was added for an additional 4-hr. The cells were washed twice with advanced DMEM media and fixed in the dish using a solution of 2% (w/v) glutaraldehyde, 4% (w/v) paraformaldehyde, in 0.1M sodium cacodylate buffer overnight at RT. The cells were then washed in 0.1 M sodium cacodylate buffer (pH 7.4) 3X5 min, post-fixed for 60 min in 1% (w/v) 1% Osmium Tetroxide in 0.1 M sodium cacodylate buffer, washed in sodium cacodylate buffer 2X5 min and Maleate buffer (pH5.1) once, 5 min, and then incubated in 1% (w/v) aqueous uranyl acetate in Maleate buffer for 60 min, followed wash in Maleate buffer 3X5 min. The cells were removed from the dish in 2:1 propylene oxide and incubated overnight in a 1:1 mixture of propylene oxide. The samples were subsequently embedded in TAAB Epon and polymerized at 60°C for 48 h. Ultrathin sections (~90 nm) were cut on a Reichert-Jung Ultracut E microtome, placed onto copper grids, stained with Uranyl acetate and Lead citrate, and then examined under 300KV at FEI Tecnai F30 and the Gatan CCD digital micrograph. Electron microscopic sample preparation and imaging was performed in conjunction with the Advanced Electron Microscopy facility at the University of Chicago.

Abbreviations

ABC: activated B-cell; CCD: charge-coupled device; DLBCL: diffuse large B-cell lymphoma; DMEM: Dulbecco's modified Eagle medium; DMSO: dimethyl sulfoxide; DTT: dithiothreitol; EC50: half-maximal concentration of drug; EGTA: ethylene glycol-bis(β-aminoethyl)-N,N,N',N'-tetraacetic acid; FACS: fluorescence-activated cell sorter; GCB: germinal center B-cell; GFP: green-fluorescent protein; HEPES: 4-(2-hydroxyethyl)-1-piperazineethanesulfonic acid; Hr: hour; MEF: mouse embryonic fibroblast; Min: minute; mM: millimolar; MOMP: mitochondrial outer membrane permeabilization; NEAA: non-essential amino acids; nM: nanomolar; PAGE: polyacrylamide gel electrophoresis; PBS: phosphate buffered saline; RPMI: Roswell Park Memorial Institute medium; RT: room temperature; SDS: sodium dodecyl sulfate; SEM: standard error of the mean; µM: micromolar; WT: wild-type.

Author contributions

AH – study design, data acquisition, data analysis and interpretation, drafting manuscript, final approval of manuscript; GKS – data acquisition, data analysis and interpretation, final approval of manuscript; MRS – acquisition of data, chemical engineering of compounds, final approval of manuscript; LR – acquisition of data, data analysis and interpretation, final approval of manuscript; MVT – data analysis and interpretation, final approval of manuscript; JLL – study design, data analysis and interpretation, drafting manuscript, final approval of manuscript.

ACKNOWLEDGMENTS

The authors would like to thank the laboratories of Loren D. Walensky, Joseph T. Opferman, and Margaret A. Shipp for graciously providing the cell lines and initial SAHB constructs, the laboratory of Andreas Strasser for the lentiviral *Bim* vectors, and the Advanced Electron Microscopy facility at the University of Chicago for assistance in acquiring the TEM images used in this study.

CONFLICTS OF INTEREST

The authors report no conflicts of interest.

FUNDING

This work was supported by the National Institutes of Health (NIH) K08-CA151450 (JLL) and the Cancer Research Foundation (JLL). Additional support was provided by the National Center for Advancing Translational Sciences of the National Institutes of Health through Grant Number UL1 TR000430.

REFERENCES

1. Czabotar PE, Lessene G, Strasser A, Adams JM. Control of apoptosis by the BCL-2 protein family: implications for physiology and therapy. *Nat Rev Mol Cell Biol.* 2014; 15:49–63. <https://doi.org/10.1038/nrm3722>. [PubMed]
2. Delbridge AR, Grabow S, Strasser A, Vaux DL. Thirty years of BCL-2: translating cell death discoveries into novel cancer therapies. *Nat Rev Cancer.* 2016; 16:99–109. <https://doi.org/10.1038/nrc.2015.17>. [PubMed]
3. Renault TT, Elkholi R, Bharti A, Chipuk JE. B cell lymphoma-2 (BCL-2) homology domain 3 (BH3) mimetics demonstrate differential activities dependent upon the functional repertoire of pro- and anti-apoptotic BCL-2 family proteins. *J Biol Chem.* 2014; 289:26481–91. <https://doi.org/10.1074/jbc.M114.569632>. [PubMed]
4. Varadarajan S, Vogler M, Butterworth M, Dinsdale D, Walensky LD, Cohen GM. Evaluation and critical

assessment of putative MCL-1 inhibitors. *Cell Death Differ.* 2013; 20:1475–84. <https://doi.org/10.1038/cdd.2013.79>. [PubMed]

5. Vogler M, Weber K, Dinsdale D, Schmitz I, Schulze-Osthoff K, Dyer MJ, Cohen GM. Different forms of cell death induced by putative BCL2 inhibitors. *Cell Death Differ.* 2009; 16:1030–9. <https://doi.org/10.1038/cdd.2009.48>. [PubMed]
6. Leveson JD, Zhang H, Chen J, Tahir SK, Phillips DC, Xue J, Nimmer P, Jin S, Smith M, Xiao Y, Kovar P, Tanaka A, Bruncko M, et al. Potent and selective small-molecule MCL-1 inhibitors demonstrate on-target cancer cell killing activity as single agents and in combination with ABT-263 (navitoclax). *Cell Death Dis.* 2015; 6:e1590. <https://doi.org/10.1038/cddis.2014.561>. [PubMed]
7. Pécot J, Maillot L, Le Pen J, Vuillier C, Trécesson SC, Fétiveau A, Sarosiek KA, Bock FJ, Braun F, Letai A, Tait SWG, Gautier F, Juin PP. Tight Sequestration of BH3 Proteins by BCL-xL at Subcellular Membranes Contributes to Apoptotic Resistance. *Cell Rep.* 2016; 17:3347–58. <https://doi.org/10.1016/j.celrep.2016.11.064>. [PubMed]
8. Tahir SK, Yang X, Anderson MG, Morgan-Lappe SE, Sarthy AV, Chen J, Warner RB, Ng SC, Fesik SW, Elmore SW, Rosenberg SH, Tse C. Influence of Bcl-2 family members on the cellular response of small-cell lung cancer cell lines to ABT-737. *Cancer Res.* 2007; 67:1176–83. <https://doi.org/10.1158/0008-5472.CAN-06-2203>. [PubMed]
9. van Delft MF, Wei AH, Mason KD, Vandenberg CJ, Chen L, Czabotar PE, Willis SN, Scott CL, Day CL, Cory S, Adams JM, Roberts AW, Huang DC. The BH3 mimetic ABT-737 targets selective Bcl-2 proteins and efficiently induces apoptosis via Bak/Bax if Mcl-1 is neutralized. *Cancer Cell.* 2006; 10:389–99. <https://doi.org/10.1016/j.ccr.2006.08.027>. [PubMed]
10. Deng J, Carlson N, Takeyama K, Dal Cin P, Shipp M, Letai A. BH3 profiling identifies three distinct classes of apoptotic blocks to predict response to ABT-737 and conventional chemotherapeutic agents. *Cancer Cell.* 2007; 12:171–85. <https://doi.org/10.1016/j.ccr.2007.07.001>. [PubMed]
11. Phillips DC, Xiao Y, Lam LT, Litvinovich E, Roberts-Rapp L, Souers AJ, Leveson JD. Loss in MCL-1 function sensitizes non-Hodgkin's lymphoma cell lines to the BCL-2-selective inhibitor venetoclax (ABT-199). *Blood Cancer J.* 2015; 5:e368. <https://doi.org/10.1038/bcj.2015.88>. [PubMed]
12. Wenzel SS, Grau M, Mavis C, Hailfinger S, Wolf A, Madle H, Deeb G, Dörken B, Thome M, Lenz P, Dirnhofner S, Hernandez-Ilizaliturri FJ, Tzankov A, et al. MCL1 is deregulated in subgroups of diffuse large B-cell lymphoma. *Leukemia.* 2013; 27:1381–90. <https://doi.org/10.1038/leu.2012.367>. [PubMed]
13. Klanova M, Andera L, Brazina J, Svadlenka J, Benesova S, Soukup J, Prukova D, Vejmelkova D, Jaksá R, Helman K, Vockova P, Lateckova L, Molinsky J, et al.

- Targeting of BCL2 Family Proteins with ABT-199 and Homoharringtonine Reveals BCL2- and MCL1-Dependent Subgroups of Diffuse Large B-Cell Lymphoma. *Clin Cancer Res.* 2016; 22:1138–49. <https://doi.org/10.1158/1078-0432.CCR-15-1191>. [PubMed]
14. Li L, Pongtompipat P, Tiutan T, Kendrick SL, Park S, Persky DO, Rimsza LM, Puvvada SD, Schatz JH. Synergistic induction of apoptosis in high-risk DLBCL by BCL2 inhibition with ABT-199 combined with pharmacologic loss of MCL1. *Leukemia.* 2015; 29:1702–12. <https://doi.org/10.1038/leu.2015.99>. [PubMed]
 15. Mérimo D, Giam M, Hughes PD, Siggs OM, Heger K, O'Reilly LA, Adams JM, Strasser A, Lee EF, Fairlie WD, Bouillet P. The role of BH3-only protein Bim extends beyond inhibiting Bcl-2-like prosurvival proteins. *J Cell Biol.* 2009; 186:355–62. <https://doi.org/10.1083/jcb.200905153>. [PubMed]
 16. Edwards AL, Wachter F, Lammert M, Huhn AJ, Luccarelli J, Bird GH, Walensky LD. Cellular Uptake and Ultrastructural Localization Underlie the Pro-apoptotic Activity of a Hydrocarbon-stapled BIM BH3 Peptide. *ACS Chem Biol.* 2015; 10:2149–57. <https://doi.org/10.1021/acscchembio.5b00214>. [PubMed]
 17. LaBelle JL, Katz SG, Bird GH, Gavathiotis E, Stewart ML, Lawrence C, Fisher JK, Godes M, Pitter K, Kung AL, Walensky LD. A stapled BIM peptide overcomes apoptotic resistance in hematologic cancers. *J Clin Invest.* 2012; 122:2018–31. <https://doi.org/10.1172/JCI46231>. [PubMed]
 18. Reynolds C, Roderick JE, LaBelle JL, Bird G, Mathieu R, Bodaar K, Colon D, Pyati U, Stevenson KE, Qi J, Harris M, Silverman LB, Sallan SE, et al. Repression of BIM mediates survival signaling by MYC and AKT in high-risk T-cell acute lymphoblastic leukemia. *Leukemia.* 2014; 28:1819–27. <https://doi.org/10.1038/leu.2014.78>. [PubMed]
 19. Bird GH, Gavathiotis E, LaBelle JL, Katz SG, Walensky LD. Distinct BimBH3 (BimSAHB) stapled peptides for structural and cellular studies. *ACS Chem Biol.* 2014; 9:831–7. <https://doi.org/10.1021/cb4003305>. [PubMed]
 20. Bai M, Skyrilas A, Agnantis NJ, Kamina S, Tsanou E, Grepic C, Galani V, Kanavaros P. Diffuse large B-cell lymphomas with germinal center B-cell-like differentiation immunophenotypic profile are associated with high apoptotic index, high expression of the proapoptotic proteins bax, bak and bid and low expression of the antiapoptotic protein bcl-xl. *Mod Pathol.* 2004; 17:847–56. <https://doi.org/10.1038/modpathol.3800130>. [PubMed]
 21. Bosch R, Dieguez-Gonzalez R, Céspedes MV, Parreño M, Pavón MÁ, Graña A, Sierra J, Mangués R, Casanova I. A novel inhibitor of focal adhesion signaling induces caspase-independent cell death in diffuse large B-cell lymphoma. *Blood.* 2011; 118:4411–20. <https://doi.org/10.1182/blood-2011-04-345181>. [PubMed]
 22. Fitzsimmons L, Boyce AJ, Wei W, Chang C, Croom-Carter D, Tierney RJ, Herold MJ, Bell AI, Strasser A, Kelly GL, Rowe M. Coordinated repression of BIM and PUMA by Epstein-Barr virus latent genes maintains the survival of Burkitt lymphoma cells. *Cell Death Differ.* 2018; 25:241–254. <https://doi.org/10.1038/cdd.2017.150>. [PubMed]
 23. Inomata M, Tagawa H, Guo YM, Kameoka Y, Takahashi N, Sawada K. MicroRNA-17-92 down-regulates expression of distinct targets in different B-cell lymphoma subtypes. *Blood.* 2009; 113:396–402. <https://doi.org/10.1182/blood-2008-07-163907>. [PubMed]
 24. Adams CM, Mitra R, Gong JZ, Eischen CM. Non-Hodgkin and Hodgkin Lymphomas Select for Overexpression of BCLW. *Clin Cancer Res.* 2017; 23:7119–29. <https://doi.org/10.1158/1078-0432.CCR-17-1144>. [PubMed]
 25. Konopleva M, Pollyea DA, Potluri J, Chyla B, Hogdal L, Busman T, McKeegan E, Salem AH, Zhu M, Ricker JL, Blum W, DiNardo CD, Kadia T, et al. Efficacy and Biological Correlates of Response in a Phase II Study of Venetoclax Monotherapy in Patients with Acute Myelogenous Leukemia. *Cancer Discov.* 2016; 6:1106–17. <https://doi.org/10.1158/2159-8290.CD-16-0313>. [PubMed]
 26. Gavathiotis E, Suzuki M, Davis ML, Pitter K, Bird GH, Katz SG, Tu HC, Kim H, Cheng EH, Tjandra N, Walensky LD. BAX activation is initiated at a novel interaction site. *Nature.* 2008; 455:1076–81. <https://doi.org/10.1038/nature07396>. [PubMed]
 27. Bijnsdorp IV, Giovannetti E, Peters GJ. Analysis of drug interactions. *Methods Mol Biol.* 2011; 731:421–34. https://doi.org/10.1007/978-1-61779-080-5_34. [PubMed]
 28. Mérimo D, Khaw SL, Glaser SP, Anderson DJ, Belmont LD, Wong C, Yue P, Robati M, Phipson B, Fairlie WD, Lee EF, Campbell KJ, Vandenberg CJ, et al. Bcl-2, Bcl-x(L), and Bcl-w are not equivalent targets of ABT-737 and navitoclax (ABT-263) in lymphoid and leukemic cells. *Blood.* 2012; 119:5807–16. <https://doi.org/10.1182/blood-2011-12-400929>. [PubMed]
 29. Glaser SP, Lee EF, Trounson E, Bouillet P, Wei A, Fairlie WD, Izon DJ, Zuber J, Rappaport AR, Herold MJ, Alexander WS, Lowe SW, Robb L, et al. Anti-apoptotic Mcl-1 is essential for the development and sustained growth of acute myeloid leukemia. *Genes Dev.* 2012; 26:120–5. <https://doi.org/10.1101/gad.182980.111>. [PubMed]
 30. Lopez J, Bessou M, Riley JS, Giampazolias E, Todt F, Rochegue T, Oberst A, Green DR, Edlich F, Ichim G, Tait SW. Mito-priming as a method to engineer Bcl-2 addiction. *Nat Commun.* 2016; 7:10538. <https://doi.org/10.1038/ncomms10538>. [PubMed]
 31. White MJ, McArthur K, Metcalf D, Lane RM, Cambier JC, Herold MJ, van Delft MF, Bedoui S, Lessene G, Ritchie ME, Huang DC, Kile BT. Apoptotic caspases suppress mtDNA-induced STING-mediated type I IFN production. *Cell.* 2014; 159:1549–62. <https://doi.org/10.1016/j.cell.2014.11.036>. [PubMed]
 32. Perciavalle RM, Stewart DP, Koss B, Lynch J, Milasta S, Bathina M, Temirov J, Cleland MM, Pelletier S, Schuetz JD, Youle RJ, Green DR, Opferman JT. Anti-apoptotic MCL-1 localizes to the mitochondrial matrix and couples

- mitochondrial fusion to respiration. *Nat Cell Biol.* 2012; 14:575–83. <https://doi.org/10.1038/ncb2488>. [PubMed]
33. Eichhorn JM, Alford SE, Sakurikar N, Chambers TC. Molecular analysis of functional redundancy among anti-apoptotic Bcl-2 proteins and its role in cancer cell survival. *Exp Cell Res.* 2014; 322:415–24. <https://doi.org/10.1016/j.yexcr.2014.02.010>. [PubMed]
 34. El-Brolosy MA, Stainier DYR. Genetic compensation: A phenomenon in search of mechanisms. *PLoS Genet.* 2017; 13:e1006780. <https://doi.org/10.1371/journal.pgen.1006780>. [PubMed]
 35. Duprez L, Wirawan E, Vanden Berghe T, Vandenabeele P. Major cell death pathways at a glance. *Microbes Infect.* 2009; 11:1050–62. <https://doi.org/10.1016/j.micinf.2009.08.013>. [PubMed]
 36. Martinou JC, Youle RJ. Mitochondria in apoptosis: Bcl-2 family members and mitochondrial dynamics. *Dev Cell.* 2011; 21:92–101. <https://doi.org/10.1016/j.devcel.2011.06.017>. [PubMed]
 37. Chonghaile TN, Roderick JE, Glenfield C, Ryan J, Sallan SE, Silverman LB, Loh ML, Hunger SP, Wood B, DeAngelo DJ, Stone R, Harris M, Gutierrez A, et al. Maturation stage of T-cell acute lymphoblastic leukemia determines BCL-2 versus BCL-XL dependence and sensitivity to ABT-199. *Cancer Discov.* 2014; 4:1074–87. <https://doi.org/10.1158/2159-8290.CD-14-0353>. [PubMed]
 38. Anderson NM, Harrold I, Mansour MR, Sanda T, McKeown M, Nagyary N, Bradner JE, Lan Zhang G, Look AT, Feng H. BCL2-specific inhibitor ABT-199 synergizes strongly with cytarabine against the early immature LOUCY cell line but not more-differentiated T-ALL cell lines. *Leukemia.* 2014; 28:1145–8. <https://doi.org/10.1038/leu.2013.377>. [PubMed]
 39. Frismantas V, Dobay MP, Rinaldi A, Tchinda J, Dunn SH, Kunz J, Richter-Pechanska P, Marovca B, Pail O, Jenni S, Diaz-Flores E, Chang BH, Brown TJ, et al. *Ex vivo* drug response profiling detects recurrent sensitivity patterns in drug-resistant acute lymphoblastic leukemia. *Blood.* 2017; 129:e26–e37. <https://doi.org/10.1182/blood-2016-09-738070>. [PubMed]
 40. Khaw SL, Suryani S, Evans K, Richmond J, Robbins A, Kurmasheva RT, Billups CA, Erickson SW, Guo Y, Houghton PJ, Smith MA, Carol H, Roberts AW, et al. Venetoclax responses of pediatric ALL xenografts reveal sensitivity of MLL-rearranged leukemia. *Blood.* 2016; 128:1382–95. <https://doi.org/10.1182/blood-2016-03-707414>. [PubMed]
 41. Peirs S, Matthijssens F, Goossens S, Van de Walle I, Ruggero K, de Bock CE, Degryse S, Cante-Barrett K, Briot D, Clappier E, Lammens T, De Moerloose B, Benoit Y, et al. ABT-199 mediated inhibition of BCL-2 as a novel therapeutic strategy in T-cell acute lymphoblastic leukemia. *Blood.* 2014; 124:3738–47. <https://doi.org/10.1182/blood-2014-05-574566>. [PubMed]
 42. Lin KH, Winter PS, Xie A, Roth C, Martz CA, Stein EM, Anderson GR, Tingley JP, Wood KC. Targeting MCL-1/BCL-XL Forestalls the Acquisition of Resistance to ABT-199 in Acute Myeloid Leukemia. *Sci Rep.* 2016; 6:27696. <https://doi.org/10.1038/srep27696>. [PubMed]
 43. Luedtke DA, Niu X, Pan Y, Zhao J, Liu S, Edwards H, Chen K, Lin H, Taub JW, Ge Y. Inhibition of Mcl-1 enhances cell death induced by the Bcl-2-selective inhibitor ABT-199 in acute myeloid leukemia cells. *Signal Transduct Target Ther.* 2017; 2:17012. <https://doi.org/10.1038/sigtrans.2017.12>. [PubMed]
 44. Yecies D, Carlson NE, Deng J, Letai A. Acquired resistance to ABT-737 in lymphoma cells that up-regulate MCL-1 and BFL-1. *Blood.* 2010; 115:3304–13. <https://doi.org/10.1182/blood-2009-07-233304>. [PubMed]
 45. Rooswinkel RW, van de Kooij B, Verheij M, Borst J. Bcl-2 is a better ABT-737 target than Bcl-xL or Bcl-w and only Noxa overcomes resistance mediated by Mcl-1, Bfl-1, or Bcl-B. *Cell Death Dis.* 2012; 3:e366. <https://doi.org/10.1038/cddis.2012.109>. [PubMed]
 46. Levenson JD, Phillips DC, Mitten MJ, Boghaert ER, Diaz D, Tahir SK, Belmont LD, Nimmer P, Xiao Y, Ma XM, Lowes KN, Kovar P, Chen J, et al. Exploiting selective BCL-2 family inhibitors to dissect cell survival dependencies and define improved strategies for cancer therapy. *Sci Transl Med.* 2015; 7:279ra40. <https://doi.org/10.1126/scitranslmed.aaa4642>. [PubMed]
 47. Inoue-Yamauchi A, Jeng PS, Kim K, Chen HC, Han S, Ganesan YT, Ishizawa K, Jebiwott S, Dong Y, Pietanza MC, Hellmann MD, Kris MG, Hsieh JJ, et al. Targeting the differential addiction to anti-apoptotic BCL-2 family for cancer therapy. *Nat Commun.* 2017; 8:16078. <https://doi.org/10.1038/ncomms16078>. [PubMed]
 48. Ashkenazi A, Fairbrother WJ, Levenson JD, Souers AJ. From basic apoptosis discoveries to advanced selective BCL-2 family inhibitors. *Nat Rev Drug Discov.* 2017; 16:273–84. <https://doi.org/10.1038/nrd.2016.253>. [PubMed]
 49. Opferman JT. Attacking cancer's Achilles heel: antagonism of anti-apoptotic BCL-2 family members. *FEBS J.* 2016; 283:2661–75. <https://doi.org/10.1111/febs.13472>. [PubMed]
 50. Kotschy A, Szlavik Z, Murray J, Davidson J, Maragno AL, Le Toumelin-Braizat G, Chanrion M, Kelly GL, Gong JN, Moujalled DM, Bruno A, Csekei M, Paczal A, et al. The MCL1 inhibitor S63845 is tolerable and effective in diverse cancer models. *Nature.* 2016; 538:477–82. <https://doi.org/10.1038/nature19830>. [PubMed]
 51. Konopleva M, Contractor R, Tsao T, Samudio I, Ruvolo PP, Kitada S, Deng X, Zhai D, Shi YX, Sneed T, Verhaegen M, Soengas M, Ruvolo VR, et al. Mechanisms of apoptosis sensitivity and resistance to the BH3 mimetic ABT-737 in acute myeloid leukemia. *Cancer Cell.* 2006; 10:375–88. <https://doi.org/10.1016/j.ccr.2006.10.006>. [PubMed]
 52. Walensky LD, Pitter K, Morash J, Oh KJ, Barbuto S, Fisher J, Smith E, Verdine GL, Korsmeyer SJ. A stapled BID BH3 helix directly binds and activates BAX. *Molecular Cell.* 2006; 24:199–210. <https://doi.org/10.1016/j.molcel.2006.08.020>. [PubMed]

53. Horn H, Ziepert M, Becher C, Barth TF, Bernd HW, Feller AC, Klapper W, Hummel M, Stein H, Hansmann ML, Schmelter C, Moller P, Cogliatti S, et al. MYC status in concert with BCL2 and BCL6 expression predicts outcome in diffuse large B-cell lymphoma. *Blood*. 2013; 121:2253–63. <https://doi.org/10.1182/blood-2012-06-435842>. [PubMed]
54. Lenz G, Staudt LM. Aggressive lymphomas. *N Engl J Med*. 2010; 362:1417–29. <https://doi.org/10.1056/NEJMra0807082>. [PubMed]